Available online at www.sciencedirect.com

ScienceDirect

Procedia Engineering 114 (2015) 590 – 597

Procedia Engineering

www.elsevier.com/locate/procedia

1st International Conference on Structural Integrity

# Strain and damage sensing in polymer composites and nanocomposites with conducting fillers

P. Pissis[a]*, G. Georgousis[b], C. Pandis[a], P. Georgiopoulos[b], A. Kyritsis[a], E. Kontou[b], M. Micusik[c], K. Czanikova[c], M. Omastova[c]

[a]*Physics Department, National Technical University of Athens, Athens, Greece*
[b]*Mechanics Department, National Technical University of Athens, Athens, Greece*
[c]*Polymer Institute, Slovak Academy of Sciences, Bratislava, Slovakia*

**Abstract**

In polymer composites and nanocomposites with conducting fillers, conductivity changes significantly with strain and with the evolution of damage, which forms the basis for using the composite itself as sensor (self-sensing) for strain and for structural health monitoring. Less frequent is the use of capacitance sensors, where the changes of capacitance of the sample during deformation are utilized. Here we present results of recent work in the use of electrical dc measurements to monitor strain and to follow the onset and evolution of damage in selected examples of polymer composites and nanocomposites, pointing out differences in their properties. The materials we measured were PP (Poly-Propylene) filled with unfunctionalized MWCNTs (Multi Walled Carbon Nano-Tubes), SBR (Styrene Butadiene Rubber) filled with CB (Carbon Black) and PEEK (Poly-Ether-Ether-Ketone) reinforced with CFs (Carbon Fibers).


Peer-review under responsibility of INEGI - Institute of Science and Innovation in Mechanical and Industrial Engineering

*Keywords:* Health Monitoring; Nanocomposites; Polymers; PP; CNTs; MWCNTs; SBR; CB; PEEK; CF

* Corresponding author. Tel.: +30 210 772 2986; fax: +30 210 772 2932.
*E-mail address:* ppissis@central.ntua.gr


Peer-review under responsibility of INEGI - Institute of Science and Innovation in Mechanical and Industrial Engineering
doi:10.1016/j.proeng.2015.08.109

## 1. Introduction

Apart from the reinforcing effect, a common characteristic of the above-mentioned fillers is that when they have been implanted into an insulating polymer matrix, an electrically conductive polymer composite is obtained. Therefore, the intrinsic conductivity of these fillers makes them multifunctional and suitable for a wide variety of applications such as their usage as sensors for strain sensing for structural health monitoring [1]. The main concept is using the structural material itself as the sensor. This concept is also referred to as self-sensing and has the advantages of being low-cost, it can be applied to a large volume of the structural material and there is an absence of mechanical property loss. The concept is based on the monitoring of the changes in electrical conductivity in order to detect the onset, nature and evolution of dangerous deformation levels in advanced polymer-based composites. A lot of research on such nanocomposites under mechanical loading has been done concerning electrical measurements such as resistivity to examine their potential use in deformation or pressure sensors [2-4].

## 2. Fabrication of the Materials

### *2.1. PP filled with MWCNTs*

Samples with various MWCNT content were prepared by mixing of maleated PP (OREVAC 18,732) with appropriate amount of a masterbatch with 20% MWCNT (Hyperion Catalysis) in the 30mL mixing chamber of a Plasticorder kneading machine PLE 331 (Brabender, Germany) at 190ºC for 10min at a mixing speed of 35rpm. One millimeter thick slabs were prepared by compression moulding of the mixed composites using a laboratory hydraulic press SRA 100 (Fontijne, Netherlands) at 2.4MPa and 190ºC for 2min. Finally, dog-bone shaped samples with gold sputtered electrodes were created.

### *2.2. SBR with CB*

The elastomeric material employed as a matrix was SBR (SBR, Unipetrol Group, Kralupy nad Vltavou, Czech Republic), which was produced by cold emulsion polymerization, and had a styrene content of 22.5–24.5 wt%, an antioxidant content of 1–1.75 wt%, an organic acid content of 5.0–6.5 wt%, and a Mooney viscosity (1 + 40 at 100°C) of 47 to 56. SBR matrix was reinforced by CB of type Chezacarb A (Unipetrol RPA, Litvinov, Czech Republic), as a superconductive CB. The matrix was reinforced with 2, 5 10, 15 and 20 wt% of CB. Finally, gold sputtered electrodes were deposited on top of dog-bone shaped samples.

### *2.3. PEEK reinforced with CF*

The composites were prepared by UD CF of type (Hexcel IM7) at a volume content of 38% in a matrix of PEEK. The UD fibers are thrown in a solution of PEEK and then the solvent is extracted. The PEEK is compressed under cyclic shearing at 390ºC. Measurements were performed on parallelepipedic samples with length 60mm, width of 10mm and thickness of 0.15mm.

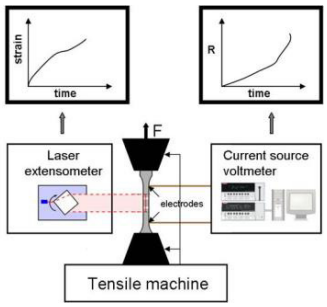


Fig. 1. Experimental Setup.

## 3. Experimental Setup

In Fig. 1 the experimental setup is depicted. Each sample was subjected to tensile loading using an Instron 1121 testing machine. The longitudinal strain was measured very accurately using a laser-extensometer which permits a non-contact measurement of the longitudinal deformation distribution of the sample. Simultaneously with the mechanical tests, the electrical resistance of the sample was monitored by applying a fixed dc current to the electrical contacts on the surface of the specimen and monitoring the voltage drop. Thus the relative voltage change ($\Delta V/V_0$) could be calculated and hence the relative resistance change ($\Delta R/R_0$) due to the constant current, where $V_0$ and $R_0$ represent respectively the initial voltage drop and the initial resistance of each sample before tension is applied. Three different configurations were used for the measurement of resistance and voltage change which are schematically presented in Fig. 2.

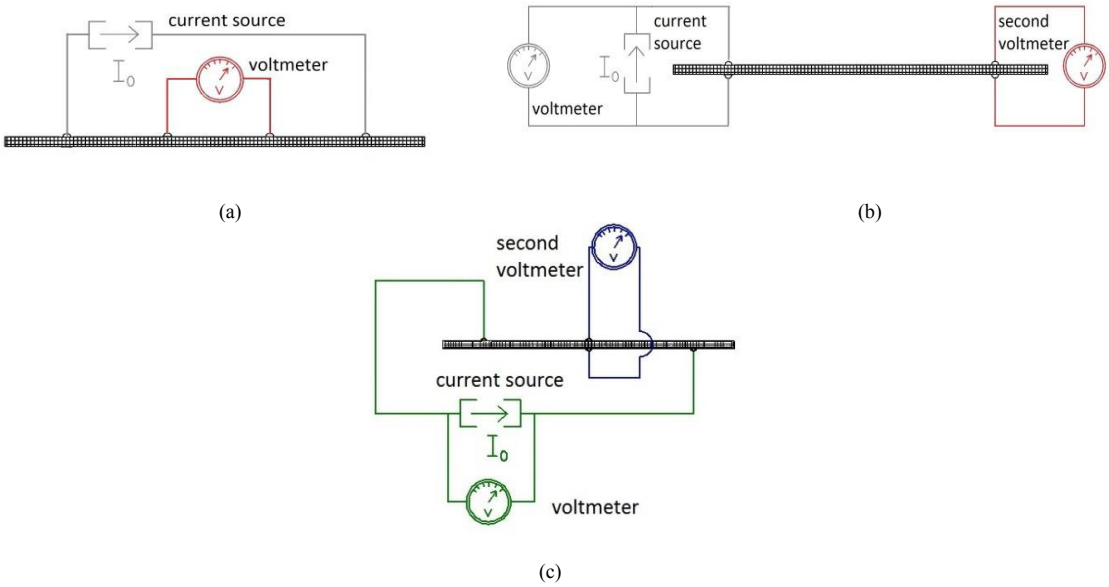


Fig. 2. Electrical contacts configuration for the measurement of resistance, (a) longitudinal, (b) through thickness, and (c) oblique resistance.

For the measurement of longitudinal resistance (Fig. 2a) a four-wire method was used by applying a fixed current through the two outer electrical contacts and measuring the voltage between the two inner electrodes. The

configuration for through thickness resistance measurement is depicted in Fig. 2b where current is applied in the two opposite contacts and the voltage drop is measured from the same wires. In the above configuration a second voltmeter was used in order to measure the voltage drop between two opposite contacts in the through thickness direction away from those for current application. The configuration for oblique resistance measurement is depicted in Fig. 2c where two contacts in the oblique direction are used for applying a fixed current and the voltage drop is measured from the same wires. In this configuration a second voltmeter is used in order to measure the voltage drop between two opposite contacts in the through thickness direction at the middle of the sample. The configuration of Fig. 2a was applied to the PP with MWCNTs and to SBR with CB samples, whereas the PEEK/CF samples were separated into three groups, where one of these three configurations was applied to each group. This was made in order to measure the electrical behavior parallel and perpendicular to the direction of the fibers.

## 4. Results and discussion

### *4.1. PP with MWCNTs*

Fig. 3 presents stress versus strain and relative resistance change $\Delta R/R_0$ versus strain for PP with 4wt% MWCNT. All preliminary mechanical tests as well as the stress-strain curve depicted in Fig. 3 showed the typical behavior of a ductile material where the linear elastic region is followed by the plastic deformation region and a neck formation before fracture. The results concerning electrical measurements showed that resistance change $\Delta R/R_0$ increases almost linearly in the elastic region, whereas when entering the plastic region $\Delta R/R_0$ changes faster up to the fracture of the specimen. This increase can be attributed to the destruction of the electrically conductive paths, because the conducting MWCNT network inside the insulating matrix rearranges itself as the elongation proceeds [5].

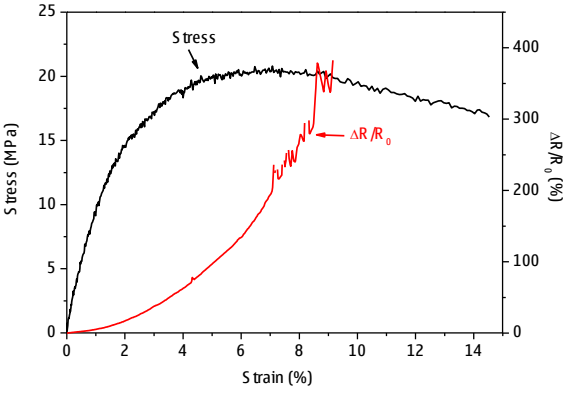


Fig. 3. Stress versus strain and $\Delta R/R_0$ versus strain for the PP with 4wt% MWCNTs.

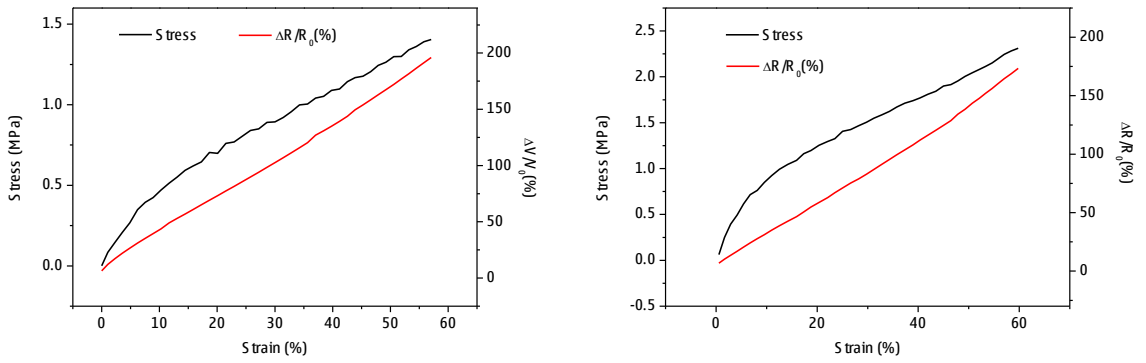


Fig. 4. Stress and $\Delta R/R_0$ against Strain for SBR with (a) 15wt% and (b) 20wt% CB.

### *4.2. SBR with CB*

The stress-strain results, plotted together with the relative resistance $\Delta R/R_0$ for samples SBR with 15 and 20wt% in CB are illustrated in Fig. 4 a and b, respectively. It must be mentioned that only the initial part of the stress-strain curves is presented here, up to 60% strain, due to the inability of the strain measurement method applied to capture the high strain values attained by the elastomers. The results concerning electrical measurements show that the curve for relative resistance change increases linearly as the elongation proceeds, for both material types examined. This linearity was maintained in the entire strain region examined. For 15wt% filler content the initial resistance was 12 kΩ and the slope is 3, which corresponds to a 75 degree angle. Samples with 20wt% CB content showed an initial resistance of 800 Ω and a slope of 2.6, which corresponds to an angle of 69 degrees. This $\Delta R/R_0$ increment with strain can be attributed to the destruction and rearrangement of the electrically conducting CB network inside the insulating matrix [6]. It must also be noticed that for the two CB loadings the slope of the curves is quite similar, and probably this could be generalized for these material types by further experimental study.

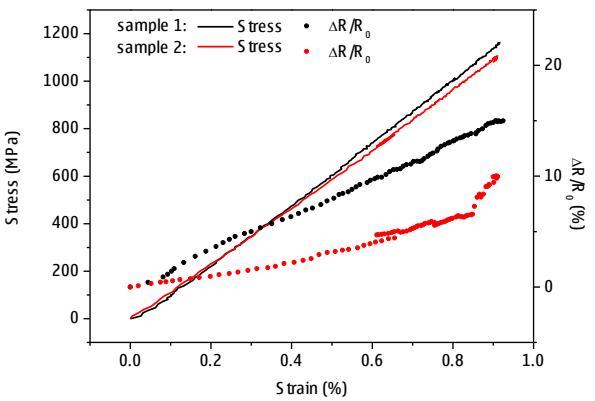


Fig. 5. Strain and $\Delta R/R_0$ measured at the longitudinal configuration versus strain for PEEK/CF.

### 4.3. PEEK with CF

In Fig. 5 results for PEEK/CF composites at the longitudinal configuration are expressed in terms of stress and $\Delta R/R_0$ against strain. Resistance increases monotonically with strain from minimum strain. The increase of $\Delta R/R_0$ is more than 10% at fracture. In the curve corresponding to the second sample a steep increase of resistance could be observed. The above is a clear indication of fiber breakage [1].

In Fig. 6a the stress versus strain during tensile loading up to the fracture of the specimen, together with the relative voltage change $\Delta V/V_0$ measured at the through thickness direction, at two different locations perpendicular to the loading direction is depicted. The first one refers to the voltage drop measured at the contacts, used for applying the current, while the other corresponds to the voltage drop measured at the through thickness direction away from the current application. A distinction between the two responses can be observed. In Fig. 6a an initial plateau of $\Delta V/V_0$ could be observed for strain up to 0.2%. For higher strain, $\Delta V/V_0$ measured at current contacts increases monotonically up to the fracture of the specimen. Contrary, in the curve corresponding to the measurement of $\Delta V/V_0$ away from current application, a slight decrement is observed. This behavior may be analyzed in terms of competing Poisson effects and fiber alignment within the specimen. However, for the interpretation of these results in relation to damage, the different conditions of the two measurements should be taken into account.

In Fig. 6b the stress versus strain during tensile loading in the fiber direction up to the fracture of the specimen is presented. In the same plot the relative voltage change $\Delta V/V_0$ measured at the oblique direction at the contacts used for applying current as well as at the through-thickness direction at the middle of the specimen is depicted. An almost monotonic increment of $\Delta V/V_0$ in the oblique direction is observed up to fracture. Regarding the $\Delta V/V_0$ values of through thickness in the middle of the specimen, a negligible change is observed up to 0.8% strain followed by a decrease up to the fracture.

In all experiments, using different configurations, an increase of resistance change upon loading was observed when voltage drop was measured by the same contacts which served for current injection. In general, the increase in the resistance during tensile loading is ascribed to (i) the load-dependence of the surface resistivity, (ii) geometrical change, and (iii) destruction of the conductive paths, such as fiber breakage and the reduction in the contact area of each fiber due to deformation and/or damage [7].

At low strains the effect of (i) and (ii) is dominant while (iii) is more pronounced at higher strains. Our results indicate that measurement in the longitudinal direction is more sensitive to fiber breakage while measurement in the through thickness direction leads to higher $\Delta V/V_0$ upon tensile loading. The increase of resistance measured in line with current application observed in our experiments, is more straightforward and is consistent with the behavior reported by the majority of works regarding strain and damage sensing by electrical measurements [7-9]. Nevertheless there is still a discrepancy and the mechanism is not fully understood.

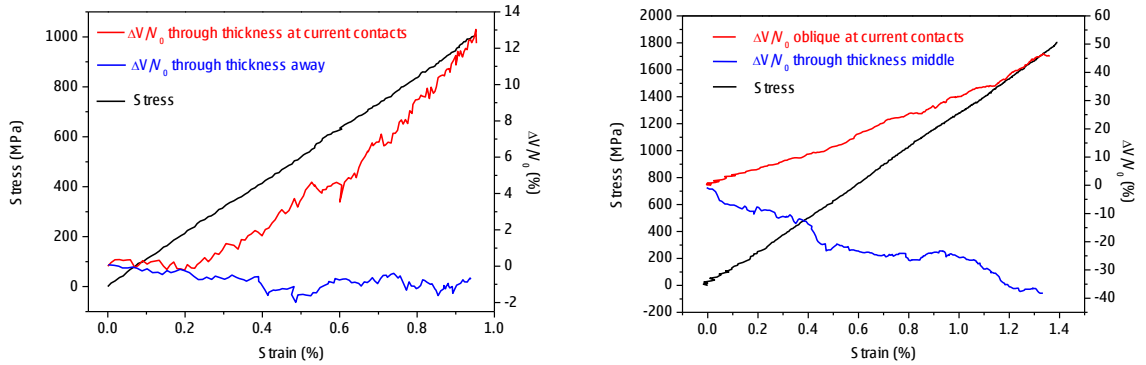


(a) (b)

Fig. 6. Stress and $\Delta V/V_0$ versus strain measured in PEEK/CF (a) at the through thickness configuration and (b) with the oblique configuration.

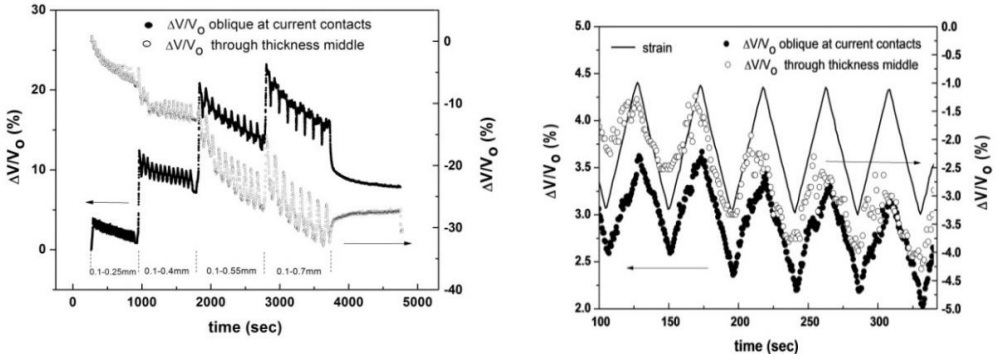


Fig. 7. (a) $\Delta V/V_0$ measured at the oblique configuration for PEEK/CF versus time of the sample subjected to tensile cyclic loading at different maximum strain levels (b) focus on 5 cycles.

### *4.4. PEEK with CF under cyclic loading*

Fig. 7 shows the resistance change measured at the oblique configuration during cyclic loading between the displacements indicated on the plot. The $\Delta V/V_0$ measured at the current contacts on the oblique direction and at the through thickness direction at the middle of the specimen are presented in the same plot. For the oblique measurement an increase of the $\Delta V/V_0$ up to about 5% is observed. After the first cycle, the viscoelastic deformation developed during cyclic loading results in an increase of resistance change at the unloaded state. The above finding implies that there is an irreversible damage during the first cycle that could be attributed to the permanent damage of the matrix [10]. However, the $\Delta V/V_0$ is reversible in the consecutive cycles. The resistance after the second cycle is recovered back to the level after the first cycle and a slight decrease of resistance level at the minimum strain is observed. The above behavior is also observed when the maximum displacement of every cycle is set to higher values. Contrary, the $\Delta V/V_0$ measured at the through-thickness direction shows a decrease upon increase of stress. The reversible change of resistance on every cycle is seen in Fig. 7b focusing on five cycles. Furthermore, a slight decrease of $\Delta V/V_0$ at the minimum loading is observed that may be attributed to relaxation processes.

### *4.5. Gauge Factor*

The following quantity GF is referred to in bibliography as the gauge factor [11], where ε is the strain.

$$GF = \frac{\Delta R}{R_0 \varepsilon} \qquad (1)$$

The SBR with CB samples showed linear electrical behavior for strain values up to 60%. Consequently these samples showed constant GF which is equal to the slope of the red lines at Fig. 4. So, for the linear part, SBR with 15wt% and 20wt% CB showed a GF of 3 and 2.6 respectively. The linear trend obtained in the strain range examined may significantly change at higher strain values. Similarly, PEEK/CF samples with the longitudinal configuration showed almost linear electrical behavior until fiber breakage. Consequently, the GF of PEEK/CF samples showed some small fluctuations, but it could be estimated to be about 11 until fibers begin to break. As far as the other two configurations are concerned, the GF is not constant. On the other hand, PP/MWCNTs samples did not show any linear electrical behavior even in the small strain regime. Consequently, their gauge factor is increasing progressively as the elongation proceeds.

## 5. Conclusion

The SBR/CB and the PEEK/CF samples showed a linear electrical behavior and a constant GF throughout their elastic region. This behavior makes these materials a good choice for use at strain sensing applications. PEEK/CF showed higher GF than SBR/CB, significantly higher maximum stress, but much lower strain at fracture, as it was expected. This makes PEEK/CF more sensitive because for a very slight strain increment, $\Delta R/R_0$ exhibits a substantial increase compared to SBR/CB due to their higher GF. Moreover, PEEK/CF is more suitable as structural material due to its higher strength than SBR/CB. However, when the material is expected to undergo high deformation levels, then SBR/CB is more suitable than PEEK/CF, as it can withstand to significantly higher strain values without yielding or losing its linear electrical behavior. On the other hand, PP with MWCNTs could be used for strain sensing applications too, because its $\Delta R/R_0$ against strain increases monotonically. However this increase is not linear and subsequently the GF is not constant making more complex to calibrate a sensor made from this material. Despite that, it could be used in cases where the other two are not suitable, because its mechanical properties lie between those of the other two materials. For example, it has higher strength than SBR/CB and can withstand higher deformation than PEEK/CF.

## Acknowledgements

This research has been co-financed by the European Union (European Social Fund-ESF) and Greek national funds through the Operational Program "Education and Lifelong Learning" Research Program Aristeia (P.P., E.K. and A. K.) and by the European Regional Development Fund, the Greek General Secretariat of Research and Technology and the Slovak Research and Development Agency in the frame of bilateral cooperation between Slovakia and Greece (APVV SK-GR-0029-11). It has been also partially supported by project VEGA 2/0149/14 (Slovakia).

## References

[1] K. Schulte, C. Baron, Load and failure analyses of CFRP laminates by means of electrical resistivity measurements, Compos. Sci. Technol. 36 (1989) 63-76.
[2] M. Knite, V. Teteris, A. Kiploka, J. Kaupuzs, Polyisoprene –Carbon Black Nanocomposites as Tensile Strain and Pressure Sensing Materials, Sens. Actuat. A 110 (2010) 142-149.
[3] T. Yasuoka, Y. Shimamura, A. Todoroki, Patch-type Large Strain Sensor Using Elastomeric Composite Filled with Carbon Nanofibers, Int. J. Aeronaut. & Space Sci. 14 (2013) 146-151.
[4] G. Georgousis, C. Pandis, A. Kalamiotis, P. Georgiopoulos, A. Kyritsis, E. Kontou, P. Pissis, M. Micusik, K. Czanikova, J. Kulicek, M. Omastova, Strain Sensing in Polymer/Carbon Nanotube Composites by Electrical Resistance Measurement, Compos. B 68 (2015) 162-169.
[5] M. Nofar, S. V. Hoa, M. D. Pugh, Failure detection and monitoring in polymer matrix composites subjected to static and dynamic loads using carbon nanotube networks, Compos. Sci. Technol. 69 (2009) 1599-1606.
[6] K. Yamaguchi, J. J. C. Busfield, A. G. Thomas, Electrical and Mechanical Behavior of Filled Elastomers, I. The Effect of Strain, J. Polym. Sci. Part B Polym. Phys. 41 (2003) 2079–2089.
[7] K. Ogi, Y. Takao, Characterization of piezoresistance behavior in a CFRP unidirectional laminate, Compos. Sci. Technol. 65 (2005) 231-239.
[8] M. Kupke, K. Schulte, R. Schuler, Non-destructive testing of FPR by d.c. and a.c. electrical methods, Compos. Sci. Technol. 61 (2001) 837-847.
[9] J. Wen, Z. Xia, F. Choy, Damage detection of carbon fiber reinforced polymer composites via electrical resistance measurement, Compos. B 42 (2010) 77-86.
[10] Z. Mei, V. H. Guerrero, D. P. Kowalik, D. D. L. Chung, Mechanical damage and strain in carbon fiber thermo-plastic-matrix composite sensed by electrical resistivity measurement, Polym. Compos. 23 (2002) 425-432.
[11] A. S. Kaddour, F. A. R. Al-Salehi, S. T. S. A1-Hassani, M. J. Hinton, Electrical Resistance Measurement Technique for Detecting Failure in CFRP Materials at High Strain Rates, Compos. Sci. Technol. 51 (1994) 377-385.